CHAPTER FIVE

ENERGY STORAGE AND CONVERSION MODELS

Madame, bear in mind
That princes govern all things|except the wind.

|Victor Hugo, \The Infanta's Dream"

Hybrid power systems employ a diversity of electrical generation sources, including intermittent sources. Energy storage and conversion devices are required to integrate these various devices into a single system able to serve a load. Power conversion devices (rectifiers and inverters) are necessary to bridge AC and DC generation sources. Most often, converters are used to connect DC batteries and PV modules to the AC bus. Energy storage allows more strategic flexibility in the dispatching of the various energy sources. Relatively small amounts of storage allow the diesel generation time to start up if an intermittent source reduces its output and is unable to meet apparent demand. Greater amounts of storage allow for strategies based on longer time intervals.

5.1 Storage Battery Models

Storage batteries are based on an *equivalent circuit model* represented in Figure 5.1, which relates the voltage, current and state-of-charge*, SOC,* of the battery. In the figure, *Rc* and *Rd* are the internal resistances to charge and discharge, respectively. *Ec* and *Ed* are the *extrapolated constant open circuit voltages* defined by Shepard (1965). The diodes, introduced by Peterson and Zimmerman (1970), represent low-current operation of the circuit.

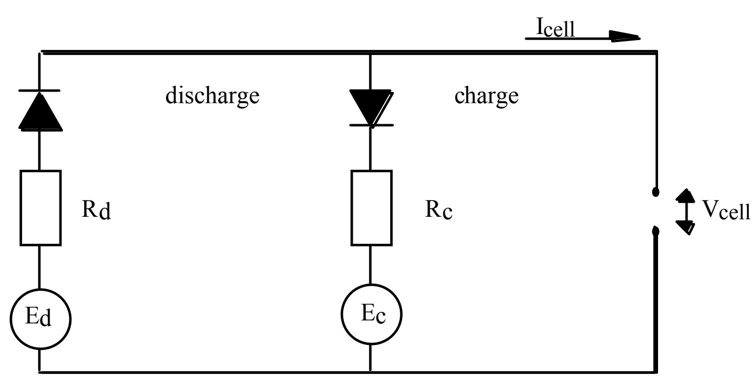

Figure 5.1 Equivalent circuit model of a storage battery.

5.1.1 *Previous Storage Battery Models*

The battery storage model used in a PV system simulation by Furler (1993), based on the Shepard/Peterson/Zimmerman (SPZ) model written as a TRNSYS Type by

Eckstein (1990 is a good representation of previous battery storage models, and is briefly summarized in this section.

The open circuit cell voltage of the SPZ model is described by

$$V_{oc} = \frac{E_c + E_d}{2} \tag{5.1}$$

The voltage drop across the diodes in the SPZ model is expressed as

$$V_{di} = \frac{1}{K_{di}} \ln \left(\frac{|I_{cell}|}{I_{di}} + 1\right) \tag{5.2}$$

where K_{di}, I_{di} are curve fitting parameters, and I_{cell} is the cell current. During charging mode, the cell voltage, V_{cell}, can be expressed as a function of the cell current, I_{cell},

$$V_{cell} = V_{oc} + V_{di} - G_c(1 - SOC) + I_{cell} R_c \left\{ 1 + \frac{m_c(1 - SOC)}{\frac{Q_c}{Q_m} - (1 - SOC)} \right\} \tag{5.3}$$

and during discharge, V_{cell} is expressed as

$$V_{cell} = V_{oc} - V_{di} - G_d(1 - SOC) + I_{cell} R_d \left\{ 1 + \frac{m_d(1 - SOC)}{\frac{Q_d}{Q_m} - (1 - SOC)} \right\} \tag{5.4}$$

where Q_c, Q_d are capacity parameters; Q_m is the rated capacity of the cell; m_c, m_d are cell type parameters; R_c, R_d are the internal resistances at full charge; and G_c, G_d are small valued coefficients of SOC. SOC is the fractional state of charge, $SOC = Q/Q_m$.

The total internal resistance of the battery cell, *R*, is expressed as a function of the internal resistance and the SOC. When the battery is fully charged *(SOC=1)*, the total internal resistance, *R*, is equal to the total resistance,

$$R = R_{c,d}\left\{1+\frac{m_{c,d}(1-SOC)}{\frac{Q_{c,d}}{Q}-(1-SOC)}\right\} \tag{5.5}$$

Figure 5.2 shows the cell voltage as a function of SOC and current based on the SPZ model.

The change in *SOC* is a linear function of battery current, where η is the charging efficiency of the battery. The discharge efficiency is assumed to be 100% and the charging efficiency is assumed to be constant. The energy losses associated with overcharging are calculated as $P_{loss} = (1 - \eta)\, P$ where P is the input energy. Since charging efficiency in the model is assumed to be constant, then the losses due to overcharging must be proportional to charge rate, which is a simplification. Losses due to overcharging are non-linear and increase with both charge rate and SOC, to the point that at SOC = 1, charging efficiency must fall to zero, by definition.

5.1.2 *Improved Storage Battery Model*

The storage battery model of Section 5.1.1 does not include the effect of variable ambient temperature or severe overcharging. Hybrid systems are often located in very hot or cold climates where temperature effects are important. In addition, more accurate overcharging models have been published.

The improvements made to the SPZ models as a part of this work are:

- Inclusion of a temperature influence on discharge capacity, and
- Charge efficiency dependency on charging rate.

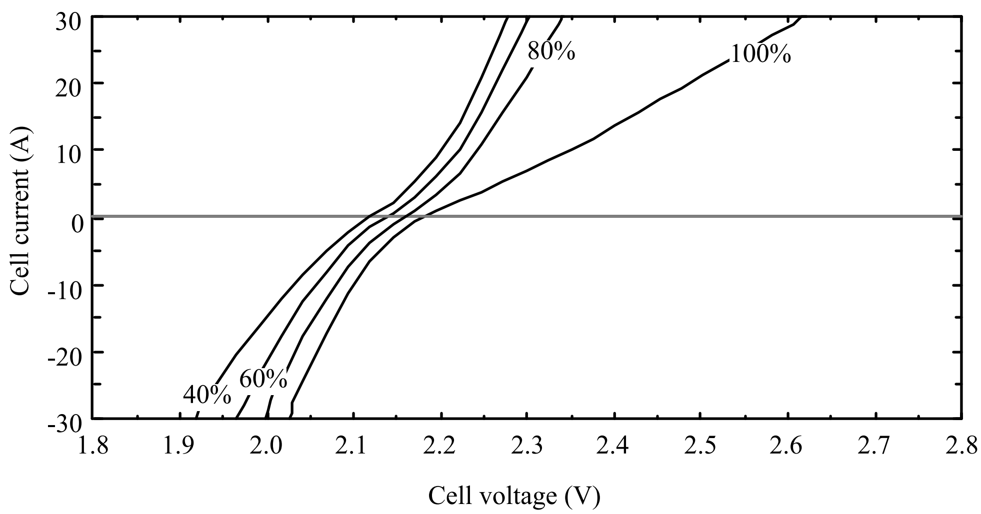

Figure 5.2 Cell current as a function of voltage, based on the SPZ model. Each line represents a different state of charge, from 60% to 100%.

Coppetti, et al (1993) at CIEMAT, the Institute for Renewable Energy Studies in Madrid Spain, recently published new battery models based on their laboratory testing program. In their work, formulations for temperature effects and overcharging were developed. The CLC model (named for the three authors of the CIEMAT paper) includes the following model for the expression of temperature effect on discharge capacity,

$$\frac{C}{C_{10}} = \frac{1.67}{1 + 1.067\left(I/I_{10}\right)^{0.9}}\left(1 + 0.005\Delta T\right) \tag{5.6}$$

where C is the capacity at the I rate of discharge, C_{10} is the ten-hour capacity, I_{10} is the current at the ten-hour rate, and $\Delta T = (T_{C^\circ} - 25^\circ C)$.

The CLC model also includes an overcharge (gassing), model. The overcharge calculation in the CLC model is performed using four equations. A final charge voltage, V_{ec} is calculated as

$$V_{ec} = \left[2.45 + 2.011 \ln\left(1 + I/C_{10}\right)\right](1 - 0.002\Delta T) \qquad (5.7)$$

A similar expression for the *gassing* voltage, V_g, is

$$V_g = \left[2.24 + 1.97 \ln\left(1 + I/C_{10}\right)\right](1 - 0.002\Delta T) \qquad (5.8)$$

Overcharging is represented in the CLC model by an exponential function incorporating V_{ec} and V_g from equations 5.7 and 5.8,

$$V_c = V_g + (V_{ec} - V_g)\left[1 - \exp\left(\frac{A\,h_{restored} - 0.95C}{I\zeta}\right)\right] \qquad (5.9)$$

where $A\,h_{restored}$ represents the Ampere-hours stored in the battery with regard to the I and C at that hour. The time constant, ζ, is in turn a function of the ten-hour battery capacity, or

$$\zeta = \frac{17.3}{1 + 852\left(\frac{I}{C_{10}}\right)^{1.67}}$$

(5.10)

Both the temperature effect equation and overcharge equations in the CLC model are incorporated into the SPZ model in order to improve the accuracy of the SPZ model when used for hybrid systems operating under extreme temperatures and during overcharging. Figure 5.3 illustrates how the CLC model varies discharge voltage as a function of temperature. The SPZ model is not sensitive to temperature, whereas the CLC component includes a temperature influence, as shown in Figure 5.3. Figure 5.4 illustrates the impact of discharge rate on discharge efficiency, as modeled in the CLC model. The SPZ model uses a fixed discharge efficiency, whereas the CLC model utilizes a non-linear model which (according to the authors) has been validated.

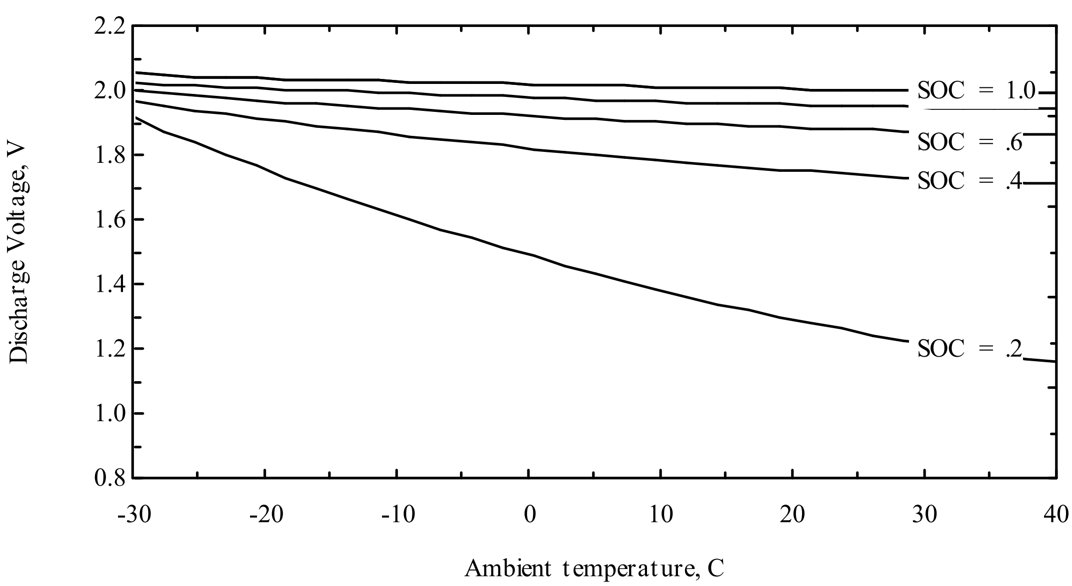

Figure 5.3 CLC modeling of discharge voltage as a function of temperature and *SOC*.

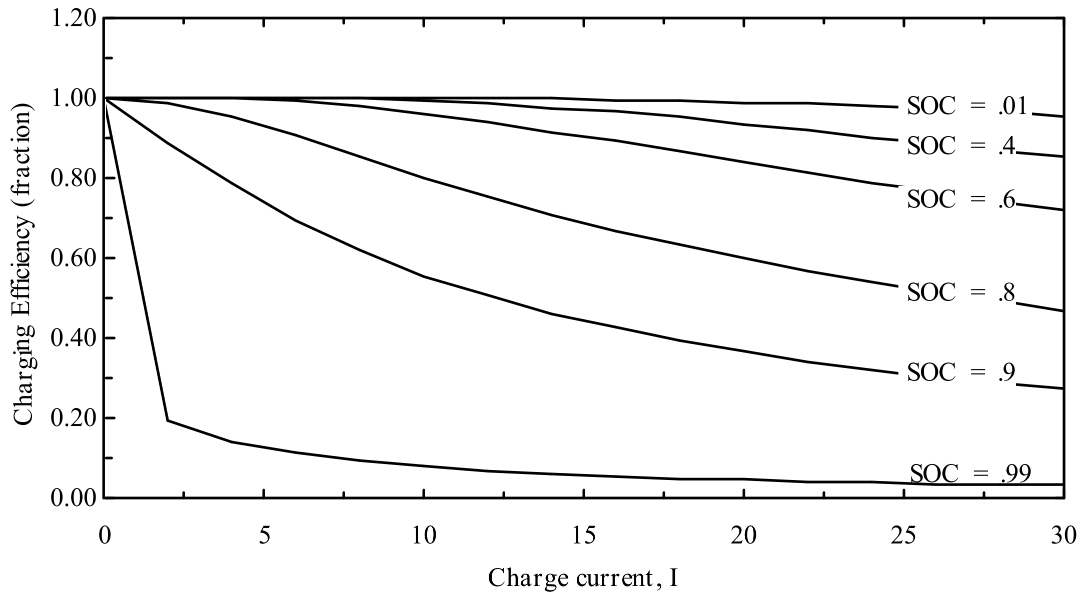

Figure 5.4 CLC modeling of charging efficiency as a function of charge rate and *SOC* for a 100 Ah capacity battery.

5.1.3 *TRNSYS Type 70: Storage Battery*

TRNSYS Type 70 is based on TRNSYS Type 74 as described by Furler (1993), with two modifications: a temperature compensation function and a function to vary charging efficiency with charge rate. The information flow diagram for Type 70 Storage Battery is shown in Figure 5.5. Eckstein (1990) and Furler (1993) provide detailed information on the determination of input parameters for Type 70 (referred to in the references as Type 74). TRNSYS Types 70 (and 74) may be used with a TRNSED interface which conveniently applies the proper parameters for the selected battery.

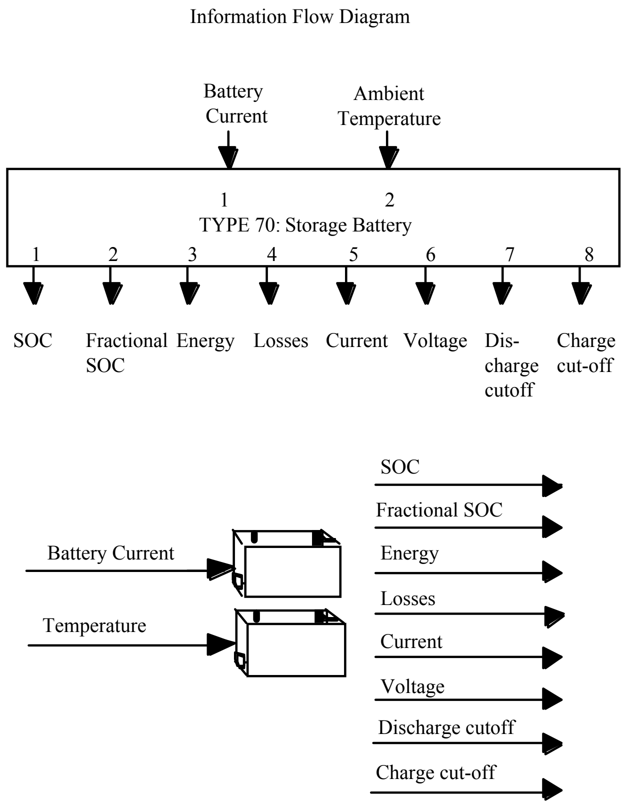

Inputs:

1.	Ibat	battery current
2.	T	temperature

Outputs:

1.	Q	state of charge
2.	SOC	fractional state of charge
3.	P	power
4.	Ploss	power losses
5.	Ibat	battery current
6.	Vbat	battery voltage
7.	Vd	cutoff voltage on discharge
8.	Vc	cutoff voltage on charge

Parameters:

1.	QM	rated capacity
2.	Cp	cells in parallel
3.	Cs	cells in series
4.	h	charging efficiency, a constant
5.	Vc	cutoff voltage on charge
6.	Vcontr	discharge cutoff voltage
7.	Ic,tol	iterative parameter
8.	Ec	open circuit charge voltage
9.	Ed	open circuit discharge voltage
10.	Gc	small valued coefficient of F
11.	Gd	small valued coefficient of F
12.	Mc	I-V cell type parameter
13.	Md	I-V cell type parameter
14.	ED	battery constant
15.	RD	battery constant
16.	Idi	curve fitting parameter
17.	Kdi	curve fitting parameter
18.	Qc	capacity parameter on charge
19.	Qd	capacity parameter on discharge
20.	Rc	internal resistance on charge
21.	Rd	internal resistance on discharge

Figure 5.5 TRNSYS Type 70: Storage Battery

The inputs, outputs parameters for Type 70 are listed below:

Inputs:

1. I_{bat} battery current
2. T temperature

Outputs:

1. Q state of charge
2. SOC fractional state of charge
3. P power
4. P_{loss} power losses

5. I_{bat} battery current
6. V_{bat} battery voltage
7. V_d cutoff voltage on discharge
8. V_c cutoff voltage on charge

Parameters:

1. Q_M rated capacity
2. C_p cells in parallel
3. C_s cells in series
4. η charging efficiency, a constant
5. V_c cutoff voltage on charge
6. V_{contr} discharge cutoff voltage
7. $I_{c,tol}$ iterative parameter
8. E_c open circuit charge voltage
9. E_d open circuit discharge voltage
10. G_c small valued coefficient of F
11. G_d small valued coefficient of F
12. M_c I-V cell type parameter
13. M_d I-V cell type parameter
14. E_D battery constant
15. R_D battery constant
16. I_{di} curve fitting parameter
17. K_{di} curve fitting parameter
18. Q_c capacity parameter on charge
19. Q_d capacity parameter on discharge
20. R_c internal resistance on charge
21. R_d internal resistance on discharge

5.2 Power Converter Models

The energy modeling of power converters deals with the efficiency of the conversion process from AC to DC (inverter) or DC to AC (rectifier). Many hybrid systems only use an inverter, while some use duel-mode inverter/rectifiers.

5.2.1 *Previous Power Converter Modeling*

Power converter performance models used at NREL are typical examples of early models which employ linear models of efficiency as a function of load (Manwell, 1996). In these models, both the rectifier and inverter are modeled identically using the following three equations:

$$P_{out} = \left(P_{in} - P_{no-load}\right)/B \tag{5.11}$$

where P_{out} = output power, P_{in} = input power, $P_{no-load}$ = no load power, and

$$B = \left(P_{rated} / \eta_{rated} - P_{no-load}\right)/P_{rated} \tag{5.12}$$

The input power to the inverter or rectifier is related to the output power by

$$P_{input} = (B)P_{output} + P_{no-load} \tag{5.13}$$

The efficiencies calculated by these equations are illustrated by the characteristic curves shown in Figure 5.6. In Figure 5.6, negative values of load indicate a rectifier mode. Maximum efficiency occurs at approximately ten percent of maximum load, and falls almost linearly between maximum efficiency and rated output. At very low loads the efficiency drops to zero.

Jennings, et al. (1996) have proposed a new normalized inverter model to be used in the RESIM (Renewable Energy Systems simulation) program under development in Australia. The Jennings model is of the form

$$\eta = \eta_{\max}\left(1 - e^{(-29P*)}\right) - 0.02P* \tag{5.14}$$

where $P* = P / P_{rated}$ is the ratio of the inverter power output to rated power output; η is the efficiency of the inverter at a given power output; and $\eta_{\max}$ is the maximum inverter efficiency.

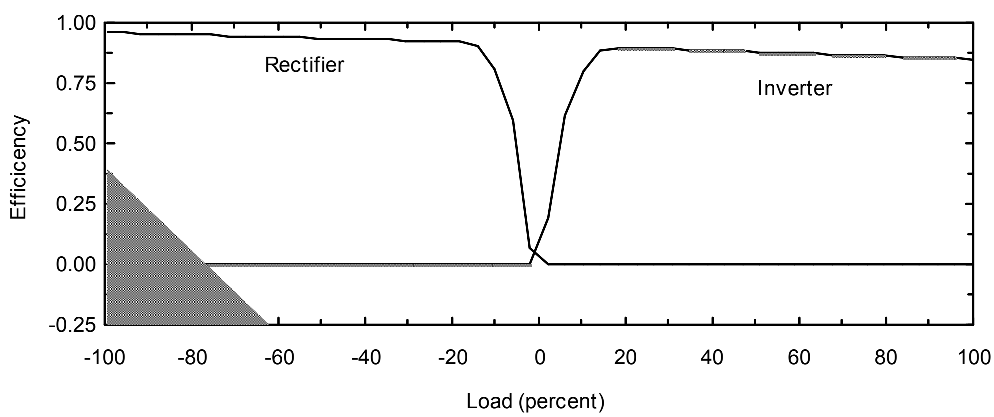

Figure 5.6 Typical efficiency curve for a dual mode (rectifier/inverter) power converter.

5.2.2 *Improved Converter Model*

Figure 5.7 shows the efficiency curves for the currently popular Trace DR series inverters. The NREL and Jennings models were compared to the inverter efficiency curves for accuracy. The Jennings model appeared to more accurately represent the output of real inverters.

The Jennings formulation uses two empirically derived numerical terms, -29 and 0.02, to characterize the shape of the function to represent inverter efficiency profiles. Since these numeric values were constraining the model to accurately represent a limited range of inverter sizes, an opportunity to improve the model was discovered. The Jennings model does not accurately estimate efficiency at rated output for all inverters. A more robust model was formulated using additional information available from the inverter specifications data:

- power output at maximum efficiency
- efficiency at rated power output

Including the additional terms, a modified Jennings model was developed, of the form

$$\eta = \eta_{no-load} + \left(\eta_{\max} - \eta_{no-load}\right)\left[\frac{P_{output} - P_{no-load}}{P_{\eta,\max} - P_{no-load}}\right]^{P_{Load}^{-0.5}} \tag{5.15}$$

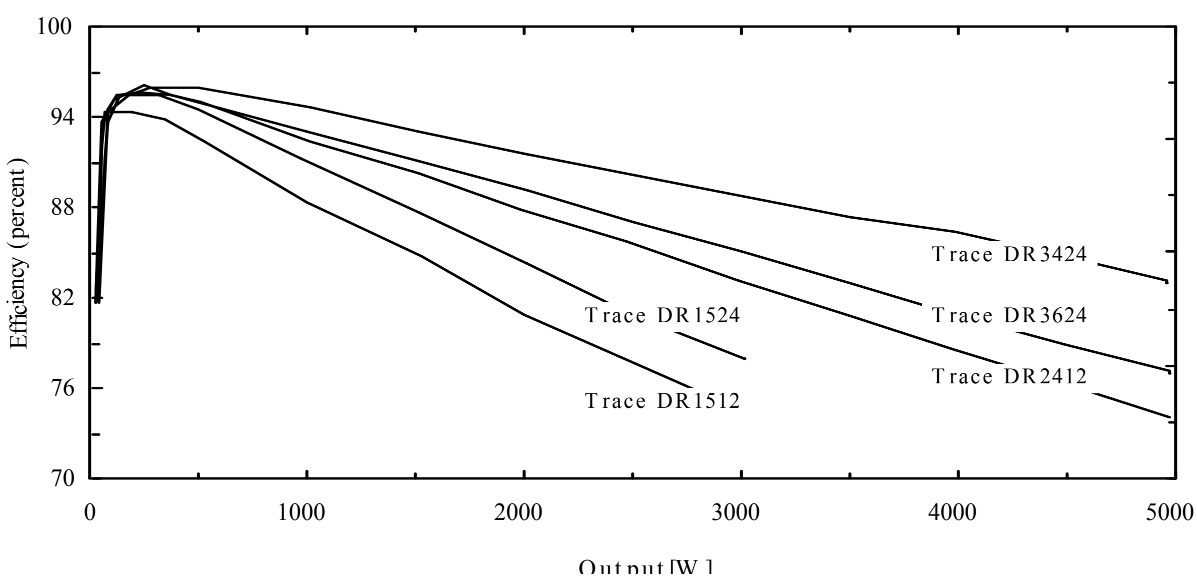

Figure 5.7 Efficiency curves for the Trace DR series inverters.

Figure 5.8 shows the different shapes of inverter output resulting from the Jennings model, modified Jennings model and the NREL model. The relative accuracy of the Modified Jennings and NREL models is assessed by plotting their efficiency estimates alongside the efficiency curve data from real inverters. Two typical inverters with published efficiency curves were selected: the Trace DR3625, and the Trace DR1512. Figures 5.9 and 5.10 show the curves produced by each model for these two inverters. The estimates produced by the modified Jennings model were in much better agreement to the manufacturer's data. In order to further investigate the fit, the results of each model were correlated to the published efficiency values, as shown in figures 5.11 and 5.12. The modified Jennings model produced superior estimates. The EES program used to develop validate the modified Jennings model is provided in Appendix A.

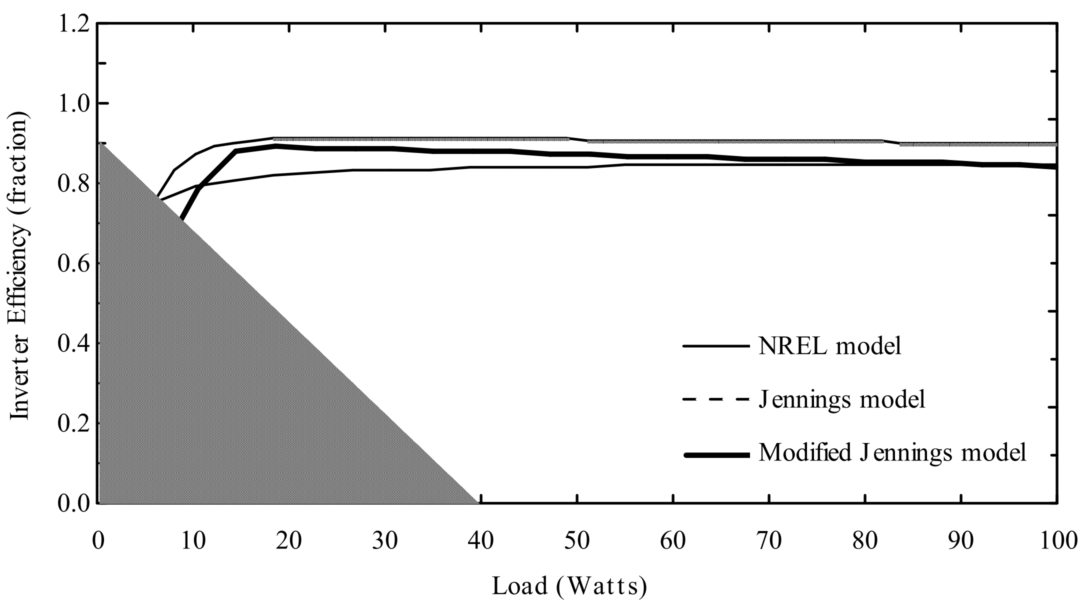

Figure 5.8 Efficiency curves produced by the modified Jennings model and NREL inverter model.

5.2.3 *TRNSYS Type 71: AC/DC Power Converter*

TRNSYS Type 71 models the energy conversion and efficiency of a dual mode, AC/DC, DC/AC power converter. For rectification, the converter uses the NREL linear model. For inverting DC to AC, the converter uses the modified Jennings model presented in section 5.2.2.

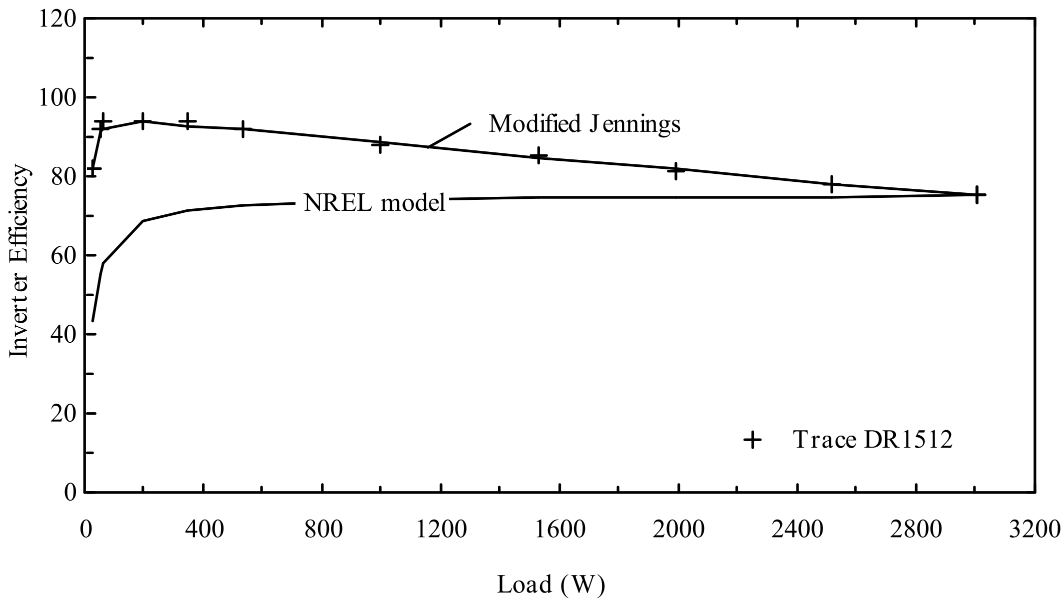

Figure 5.9 The Trace DR1512 modeled by the modified Jennings model and NREL inverter model.

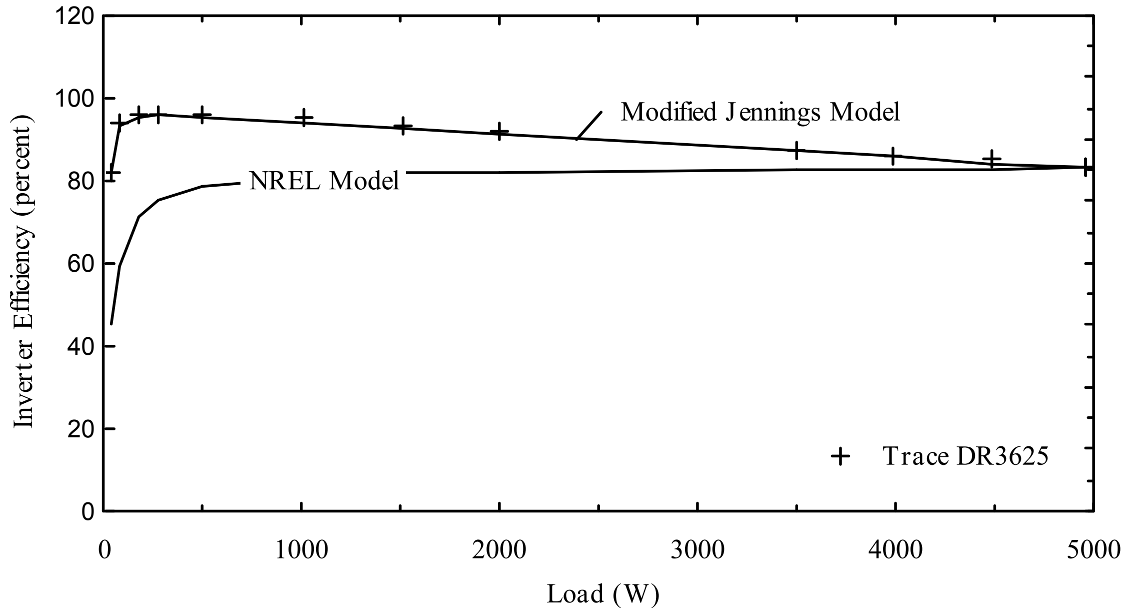

Figure 5.10 The Trace DR3625 modeled by the modified Jennings model and NREL inverter model.

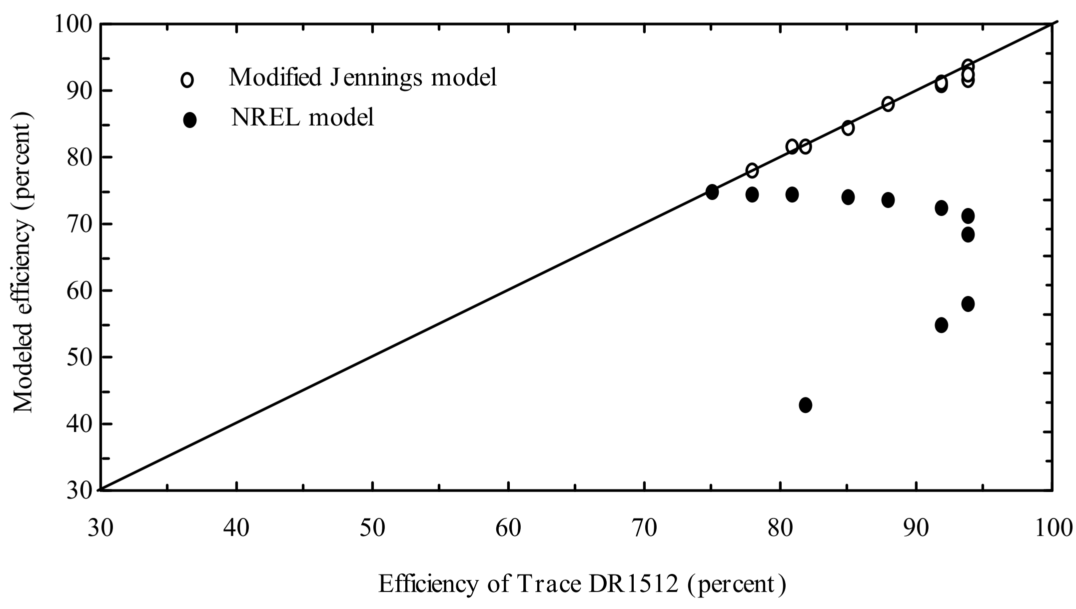

Figure 5.11 Correlation of modified Jennings model and NREL model to Trace DR1512 efficiency curve data.

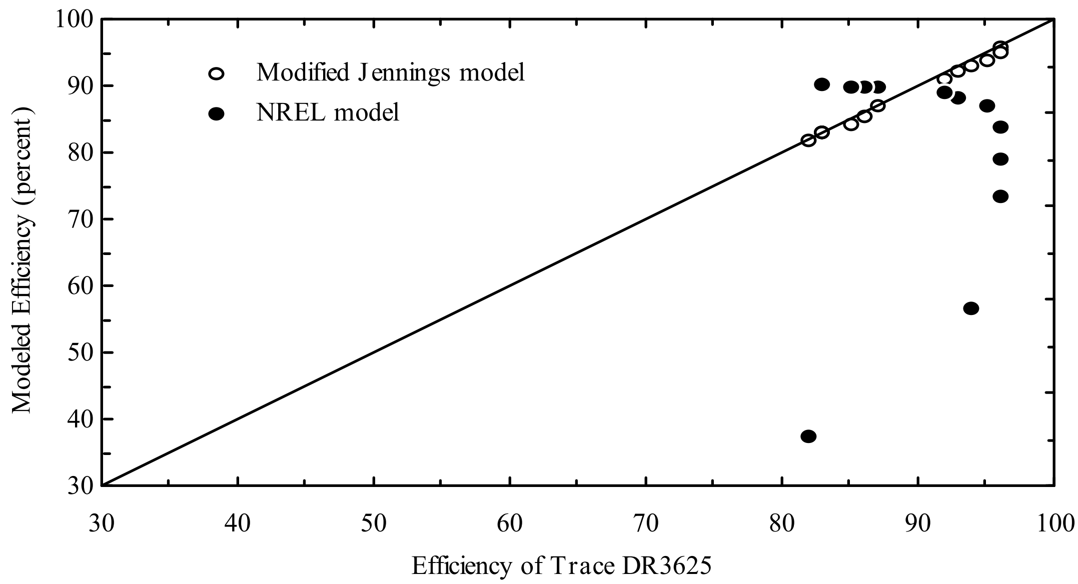

Figure 5.12 Correlation of modified Jennings model and NREL model to Trace DR3625 efficiency curve data.

Type 71 first reads in the operating parameters for the inverter, then the rectifier, as shown in the Information flow diagram for Type 71 in Figure 5.13. Type 71 uses separate specifications for each mode because the inverter and rectifier operate independently: each has its own performance characteristics. Specifying zero data for the inverter or rectifier parameters causes the model to operate in a single mode.

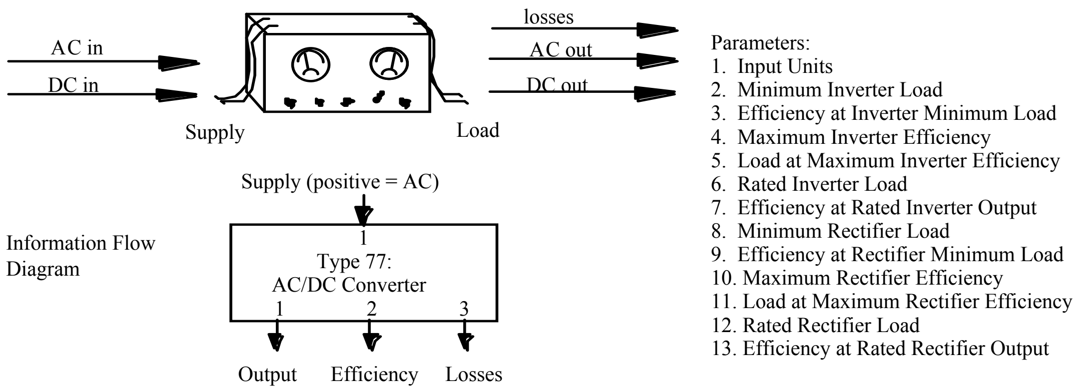

Figure 5.13 TRNSYS Type 71: Power Converter

The input to the converter is the energy input per timestep. A negative sign indicates that the converter is to operate in the rectifier mode. The output of the converter is the output energy per timestep, efficiency value, and energy losses (due to inefficiencies) per timestep. A listing of Type 71 is provided in Appendix B.